Published in final edited form as:
Microvasc Res. 2010 March ; 79(2): 93–101. doi:10.1016/j.mvr.2010.01.006.

Chronic Whole-body Hypoxia Induces Intussusceptive Angiogenesis and Microvascular Remodeling in the Mouse Retina

Alyssa C. Taylor[1], **Lara M. Seltz**[1], **Paul A. Yates**[1,2], and **Shayn M. Peirce**[1]

[1]Department of Biomedical Engineering, University of Virginia, Charlottesville, VA

[2]Department of Ophthalmology, University of Virginia, Charlottesville, VA

Abstract

Currently, little is known about the response of the adult retinal microvasculature to hypoxia. To test the hypothesis that chronic systemic hypoxia induces angiogenesis and microvascular remodeling in the adult mouse retina, adult 10-wk old female C57Bl/6 mice were exposed to 10% O_2 for 2 or 3 weeks. After hypoxia exposure, retinas were harvested, whole-mounted, and processed for immunohistochemistry. Retinas were stained with lectin, anti-smooth muscle α-actin antibody, and anti-NG2 antibody to visualize microvascular networks and their cellular components. Confocal microscopy was used to obtain images of superficial retinal networks. Images were analyzed to assess vessel diameter, vascular length density, branch point density, and the presence of vascular loops, a hallmark of intussusceptive angiogenesis. Both 2 and 3 weeks of hypoxia exposure resulted in a significant increase in the diameters of arterioles and post-arteriole capillaries ($p < 0.003$). After 3 weeks of hypoxia, vascular length density and branch point density were significantly increased in retinas exposed to hypoxia as compared to normoxic controls ($p < 0.001$). The number of vascular loops in the superficial retinal networks was significantly greater in hypoxia-exposed retinas ($p \leq 0.001$). Our results demonstrate, for the first time, intussusceptive angiogenesis as a tissue-level mechanism of vascular adaptation to chronic systemic hypoxia in the adult mouse retina and contribute to our understanding of hypoxia-induced angiogenesis and microvascular remodeling in the adult animal.

Keywords

angiogenesis; hypoxia; intussusceptive microvascular growth; microvascular remodeling; mouse; retina

Introduction

The adult retina is one of the most metabolically active tissues of the human body and is highly sensitive to changes in ambient oxygen levels (Wangsa-Wirawan and Linsenmeier, 2003). Systemic hypoxia, caused for example by chronic lung disease, congenital heart disease, or exposure to low oxygen levels from residing at high altitudes, can result in retinal hypoxia (Arjamaa and Nikinmaa, 2006; Wangsa-Wirawan and Linsenmeier, 2003). Retinal hypoxia is

Corresponding Author: Shayn M. Peirce, Department of Biomedical Engineering, P.O. Box 800759, UVA Health System, Charlottesville, VA 22908, Phone: (434) 243-5795, Fax: (434) 982-3870, smp6p@virginia.edu.

also a condition that occurs in many ocular diseases involving pathological retinal angiogenesis. For instance, both diabetic retinopathy and retinopathy of prematurity (ROP) are linked to retinal hypoxia (Arjamaa and Nikinmaa, 2006; Campochiaro, 2000; Linsenmeier et al., 1998). Pathological retinal angiogenesis is a major cause of vision loss in both infants and adults, and hypoxia is the initiating event that causes an upregulation of growth factors critical for this process, such as vascular endothelial growth factor (VEGF) (Campochiaro, 2000; Das and McGuire, 2003).

Although hypoxia is a key feature of many proliferative vasculopathies, these diseases and their established animal models also involve other factors besides hypoxia, such as inflammation, ischemia, and cellular injury stress responses (Gariano and Gardner, 2005; Smith et al., 1994). Currently, little is known about the response of the adult retinal vasculature to hypoxia alone, in the absence of other confounding disease factors. Previous work has initiated the investigation of the vascular response of the adult retina to global hypoxia, and interestingly, hypoxia was found to cause intra-retinal angiogenesis in the adult zebrafish and rat (Cao et al., 2008; Shortt et al., 2004). However, since inter-species differences in the angiogenic responses for the same stimuli have been shown to exist (Norrby et al., 1989; Pichiule and LaManna, 2002; Ward et al., 2007), the adaptations of the murine retinal microvasculature under systemic hypoxia remain to be determined. Importantly, an understanding of these adaptations would lay the foundation for studies involving genetically manipulated mice to investigate molecular mechanisms of hypoxia adaptation.

Prior work investigating the response of the adult rat retinal vasculature to chronic whole-body hypoxia relied on stereological techniques and retinal sections to assess whether or not intra-retinal angiogenesis occurred in response to chronic hypoxia (Shortt et al., 2004). Although this study provided preliminary evidence of an intra-retinal angiogenic response in rodents, the mechanism of vascular adaptation leading to this apparent hypoxia-induced angiogenic response remains to be identified. In addition, the specific vessel types undergoing remodeling (i.e. arteriole vs. venule vs. capillary), and their locations along the hierarchy of the retinal microvascular networks remain unknown. Previous work conducted in the zebrafish identified the morphological structure of hypoxia-induced retinal angiogenesis (Cao et al., 2008), but an examination of other important vascular features which contribute to vessel functionality, such as perivascular cell coverage, is still needed. To date, no other reports have been published on angiogenesis and microvascular structural changes in the adult retinal circulation in response to global hypoxia (Arjamaa and Nikinmaa, 2006).

In this study, we hypothesized that chronic systemic hypoxia would lead to angiogenesis and microvascular remodeling in murine retinal microvascular networks. Through the utilization of immunohistochemistry on whole-mounted retinal tissue, we provide a novel, detailed evaluation of the cellular features and structural network adaptations of the retinal microvasculature induced by 2 and 3 weeks of hypoxia exposure. To the best of our knowledge, this study presents, for the first time, an in-depth analysis of the vascular adaptations occurring throughout intact, whole retinal microvascular networks in the mouse in response to systemic hypoxia. Here we provide evidence, for the first time, of intussusceptive angiogenesis as a mechanism of retinal vascular adaptation to systemic hypoxia in the adult mouse.

Materials and Methods

Chronic Whole-Body Hypoxia Model

All procedures were approved by the University of Virginia's Institutional Animal Care and Use Committee (IACUC). Adult 10-wk old female C57Bl/6 mice (The Jackson Laboratory) were housed in an air-tight Plexiglass chamber for either 2 weeks or 3 weeks. Oxygen levels were lowered to 10% inside the chamber through the infusion of nitrogen controlled by a ProOx

model 350 oxygen controller (BioSpherix), as described previously (Palmer et al., 1998). An oxygen level of 10% was selected based on numerous previous studies involving chronic whole-body hypoxia in the adult animal (Cao et al., 2008; Dhillon et al., 1984; Howell et al., 2003; Miyamoto et al., 2005). Control age-matched normoxic mice were housed in the same location as the hypoxia chamber, and were exposed to the same light/dark cycles (12:12-h), temperature, and relative humidity (RH). As expected with this model (Shortt et al., 2004), mice after exposure to hypoxia weighed significantly less than their normoxic controls (mean weight = 20.7 ± 0.153 g for 3 weeks hypoxia, = 18.5 ± 0.60 g for normoxia, $p < 0.03$). Carbon dioxide and moisture in the hypoxia chamber was removed by filters via Drierite (anhydrous calcium sulfate) and activated carbon (Fisher Scientific). Mice were visually observed daily through the transparent chamber, and temperature and humidity were maintained within the required ranges of 68-72 °F and 30-60% RH. Food and water levels were checked daily, and cages were changed twice a week to supply the animals with fresh bedding, as is standard vivarium practice.

Retinal Whole-mount Procedure and Immunohistochemistry

Mice were euthanized with CO_2 inhalation. Eyes were enucleated and fixed using 4% paraformaldehyde (PFA) in phosphate-buffered saline (PBS) for 30 minutes at 4°C. Following preliminary fixation, the cornea and lens were separated from the posterior eyecup using visualization provided by a Nikon SMZ1500 stereomicroscope (Nikon Instruments). The posterior eyecup was fixed for an additional 90 minutes in 4% PFA at 4°C, and the retina was removed from the posterior eyecup and flat-mounted on a gelatin-coated slide.

In order to visualize microvascular networks and their primary cellular components, retinal tissue was stained with *Griffonia simplicifolia* isolectin B4 (GS-IB4) pre-conjugated to either Alexa Fluor 488, 568 or 647 (Invitrogen), which labels endothelial cells (Gerhardt and Betsholtz, 2003; Hansen-Smith et al., 2001). Monoclonal anti-smooth muscle α-actin (SMA) antibody pre-conjugated to either FITC or CY3 (Sigma Aldrich) was used to label smooth muscle cells (SMCs) (Saint-Geniez et al., 2003; Shortt et al., 2004; Taylor et al., 2007). Retinas were washed 4 times for 10 minutes each with 0.1% saponin/PBS at 4°C and permeabilized in 10% Triton-X 100 (Bio-Rad) for 2 hours at room temperature. Blocking of non-specific antibody binding was performed using 5% normal donkey serum (NDS) (Sigma-Aldrich) in 0.1% saponin/PBS solution for 1 hour at room temperature. The retinas were incubated overnight at 4°C with GS-IB4 (1:200) and anti-SMA antibody (1:200) conjugated to the appropriate fluorophores and diluted in antibody buffer consisting of PBS, 0.1% saponin, 2% bovine serum albumin (Jackson ImmunoResearch), and 5% NDS. Retinas were washed on the following day 8 times for 5 minutes each with 0.1% Saponin/PBS. Some retinas were additionally stained for NG2 to label pericytes (Gerhardt and Betsholtz, 2003; Taylor et al., 2007) using rabbit polyclonal anti-NG2 antibody (1:200) (Chemicon) followed by CY2-conjugated goat anti-rabbit IgG (1:200) (Jackson ImmunoResearch) in antibody buffer containing 5% normal goat serum. After washing, retinas were mounted using VectorShield (Vector Labs) and stored at 4°C.

Whole-eye Sections

Sagittal cross-sections were obtained from eyes of mice exposed to hypoxia for 3 weeks (N = 4) and their normoxic controls (N = 4). Following enucleation, eyes were fixed in 4% PFA at 4°C for 24 hours. Eyes (n = 4) were paraffin-embedded and 10 representative 5 μm-thick sagittal cross-sections were taken from the central region of each eye, approximately 40 μm apart. Samples were stained with hematoxylin and eosin (H&E), to allow for the visualization of vessel cross-sections, as well as the identification of any preretinal neovascular tufts.

Image Acquisition

A Nikon TE 2000-E2 microscope equipped with a Melles Griot Argon Ion Laser System and Nikon D-Eclipse C1 accessories was used to image whole-mounted retinal tissue. Digital confocal images of the retinal microvasculature were acquired using a 10×/0.30 DIC L/N1 dry objective and a 20×/0.75 NA Nikon oil immersion objective and Nikon EZ-C1 software (Nikon Instruments). All images were acquired using identical gain and aperture size settings on the confocal microscope. During the acquisition of both 10× and 20× images, the confocal focal plane was standardized among images by focusing on the main radially-oriented arterioles of the superficial retina. Whole-eye sections were imaged using a Nikon Eclipse 80i epifluorescence microscope with a 20×/0.50 DIC M/N2 Plan Fluor dry objective (Nikon Instruments) and Olympus Color Microfire™ Digital Camera (Olympus).

Analysis of Microvascular Remodeling

Vessel Diameter Measurements—Vessel diameter measurements were acquired from 20× confocal images of the superficial vascular network using ImageJ image analysis software (NIH). The Strahler ordering scheme (Engelson et al., 1985; Peirce et al., 2004) was used to classify vessels into different orders so that diameters of vessels of the same type and location along the retinal microvascular network could be compared. To establish vessel order, main radially-oriented arterioles were defined as vessel order 1, and sequential vessel orders were assigned progressively downstream, incrementing at branch points at which two vessels of the same order joined (Peirce et al., 2004) (see Fig. 1). The diameters were determined for first, second, third, and fourth order vessels, which encompassed main radially-oriented arterioles to post-arteriole capillaries. Vascular diameters were obtained from 3 - 9 representative fields of view (FOV) from whole-mounted retinas (n = 4) from 3 mice per experimental group. Vessel diameter measurements were performed in a blinded manner.

Vascular Length Density and Branch Point Density Measurements—Vascular length density measurements were acquired using 10× confocal images of the central to mid-peripheral superficial retinal. Representative FOV were taken containing the superficial post-arteriole networks located between radially-oriented arteriole and venule pairs. The total length (μm) of all vessels of the superficial vascular plexus contained in a defined vascular area between a main arteriole and venule pair was measured using ImageJ (NIH). The total vascular length (μm) was then divided by the defined vascular area (μm^2) to determine the vascular length density ($\mu m/\mu m^2$). Vascular length density measurements were obtained from 3 – 9 representative FOV obtained from retinas (n = 4) from 3 mice per experimental group. The number of branch points in the defined vascular area was also measured to obtain branch point density. All data analysis was performed in a blinded manner.

Analysis of Intussusceptive Angiogenesis: Loop Formation

Quantification of vascular loop formation after 2 and 3 weeks of hypoxia exposure was performed using 20× confocal images of immunolabeled superficial vascular networks. Using ImageJ, 30 representative FOV per experimental group were examined. The number of vascular loops per FOV was measured, in addition to the area encompassed by each loop (μm^2). Loop measurements were obtained from 3 – 7 FOV per retina (n = 6) from 6 mice per experimental group.

Statistical Analysis

All results are shown as the mean ± the standard error of the mean (SEM). Unless otherwise noted, N represents the number of mice studied in each group, while n represents the number of individual retinas studied in each group. To test for statistically significant differences

between the means of two groups, unpaired standard Student t-tests were used. Statistical significance was asserted at a p-value ≤ 0.05.

Results

Chronic Whole-body Hypoxia Results in Vessel Diameter Enlargement

To investigate the effects of chronic whole-body hypoxia exposure on murine retinal vasculature, adult C57Bl/6 mice were exposed to 10% environmental oxygen for a period of 2 or 3 weeks. Exposure to whole-body hypoxia for 3 weeks resulted in an increase in the diameters of arterioles and post-arteriole capillaries in the superficial networks of the adult mouse retina. Comparing normoxia to hypoxia-exposed retinas, central arterioles, as well as arterioles and capillaries of vascular networks downstream of central arterioles, of hypoxia-exposed tissue exhibited increased diameters (Fig. 1).

To quantify this apparent increase in vessel diameter, 20× confocal images from retinal tissue immunolabeled with SMA and lectin were used to measure the diameters of main arterioles and their downstream vessels. To establish vessel order, central arterioles were defined as vessel order 1, and sequential orders were assigned progressively downstream, incrementing at branch points at which two vessels of the same order joined (Peirce et al., 2004). Quantification of retinal vessel diameters demonstrated that exposure to 3 weeks of hypoxia resulted in a significant increase in the vessel diameters of central arterioles (vessel order 1), as well as downstream arterioles (the majority of which were of vessel order 2) and capillaries (the majority of which were of vessel order 3 and 4) (Fig. 2). This increase in vessel diameter was not found to correlate with an increase in SMA-positive perivascular cell investment along the arteriolar tree (Fig. 4), a hallmark of arterialization (Peirce et al., 2004; Peirce and Skalak, 2003). A significant increase in vessel diameter was also measured after 2 weeks of hypoxia for vessel orders 2, 3, and 4 ($p < 0.001$). However, the increase in central arteriole diameter (vessel order 1) was not significant after 2 weeks of hypoxia exposure (Figure 2). Confocal images were also used to examine venule diameters after 3 weeks of whole-body hypoxia exposure. No significant difference was measured in the main central radially-oriented venule diameters of normoxia versus hypoxia-exposed retinas (mean diameter = 28.5 ± 2.44, = 29.6 ± 2.23 μm respectively).

Whole-eye sections taken from mice exposed to normoxia or hypoxia further demonstrate diameter enlargement in vessels of the superficial retina after 3 weeks of hypoxia exposure (Fig. 3). In addition, whole-eye sections indicate that the angiogenic response induced by chronic whole-body hypoxia does not involve the formation of preretinal neovascular tufts that penetrate the inner limiting membrane (Fig. 3), a key feature in pathological settings of retinal angiogenesis such as the murine oxygen-induced retinopathy model of human ROP (Campochiaro, 2000;Smith et al., 1994).

Chronic Whole-body Hypoxia Induces Retinal Angiogenesis

In mice, the main central arterioles and venules of the superficial retina extend radially from the optic nerve (Gariano and Gardner, 2005) and are distributed alternately such that each main arteriole is separated by a main venule (Fig. 4). Arteriole versus venule vessel identity was determined through SMA immunostaining, as arterioles but not venules of the mouse retina express SMA (Claxton and Fruttiger, 2005; Saint-Geniez et al., 2003). To determine if intra-retinal angiogenesis was induced by hypoxia exposure, the superficial vascular plexus was examined. Immunohistochemistry performed on whole-mounted retinal tissue demonstrated that the vascular networks of the superficial retina underwent angiogenesis as a result of 3 weeks of exposure to hypoxia (Fig. 4). Retinal vascular networks from animals exposed to

hypoxia exhibited an increased amount of capillary branching (Fig. 4B) compared to vascular networks from animals exposed to normoxia (Fig. 4A).

To quantify the angiogenic response, confocal images of immunolabeled retinal tissue were used to measure the vascular length density and branch point density of superficial vascular networks. No significant difference in vascular length density was measured for mice exposed to hypoxia for 2 weeks. However, after 3 weeks of hypoxia exposure, the vasculature of the superficial retina displayed a significant increase in vascular length density (Fig. 5A) (mean vascular length density = 0.005 ± 0.0003 for normoxia, = 0.008 ± 0.0004 μm/μm^2 for hypoxia, $p < 0.001$). The mean number of blood vessel branch points in the superficial retina significantly increased after 3 weeks of hypoxia exposure (mean branch point density = 0.000035 ± 0.000002 for normoxia, = 0.000053 ± 0.000003 branch points/μm^2 for hypoxia, $p < 0.001$) (Fig. 5B). However, similarly to vascular length density, no significant change in branch point density was measured after 2 weeks of hypoxia exposure (Fig. 5B).

Perivascular Cell Coverage—To examine perivascular cell coverage, retinal tissue was immunolabeled for the perivascular cell markers NG2 proteoglycan (marker of microvascular pericytes) and SMA (a contractile protein expressed by SMCs). SMA investment appeared to be similar between normoxia and hypoxia-exposed retinal microvascular networks (Fig. 4). Immunolabeling for NG2 demonstrated the extensive pericyte coverage of retinal microvascular networks. After 3 weeks of hypoxia exposure, all microvessels detected were completely invested with pericytes, indicating that the angiogenic response induced by chronic hypoxia resulted in the formation of pericyte-invested microvasculature (Fig. 6).

Retinal Vascular Adaptations to Chronic Whole-body Hypoxia Involve Intussusceptive Angiogenesis

Although a clear hypoxia-induced angiogenic response was detected after 3 weeks of exposure (Figs. 4 and 5), the presence of blind-ended capillary sprouts was not detected in any of our retinal samples. Therefore, abluminal lateral capillary sprouting appeared to be an unlikely mechanism for the measured angiogenesis in the superficial retinal vascular network. Thus, we sought to test the hypothesis that intussusceptive luminal splitting, another mode of angiogenesis (Egginton et al., 2001), results in the increased vascular length and branching measured in this study.

Since vascular loop formation can result from intussusceptive microvascular growth (Patan et al., 2001), representative confocal images were used to quantify the number and size of vascular loops in superficial retinal networks, in order to determine whether adaptation to systemic hypoxia involves intussusceptive angiogenesis. In retinas exposed to 3 weeks of hypoxia, vascular loops of different sizes were detected, representing the progressive stages of intussusceptive microvascular growth, from the initial formation of a tissue pillar (a tissue column transversing the capillary lumen) to its subsequent elongation and expansion (Burri and Djonov, 2002) (Fig. 7). The smallest loops detected in hypoxia-exposed retinas had a diameter of 2 μm (Fig. 7A), and correspond to the size and morphology of early tissue pillars previously detected in other developing tissues (Burri and Djonov, 2002; Dunlop et al., 1997).

To quantify the extent of retinal vascular loops present after 2 and 3 weeks of hypoxia exposure, the number of loops per representative FOV was counted. The area encompassed by each loop was also measured. The number of loops per FOV was significantly greater in the retinas exposed to 3 weeks of hypoxia versus normoxic controls (mean number of loops/FOV = 0.67 ± 0.12, = 0.067 ± 0.046, respectively, $p \leq 0.001$) (Fig. 8A). Out of the 30 FOV examined for each treatment group, only 2 vascular loops were found in the 3 week normoxia-exposed retinas. However, 20 vascular loops were detected in the 3 week hypoxia-exposed retinas, and

the sizes of the loops were found to be nearly evenly distributed (Fig. 8B). After 2 weeks of hypoxia exposure, only 3 loops were detected, indicating that the intussusceptive angiogenic response occurred between 2 and 3 weeks of hypoxia-exposure (Fig. 8B). Based on the notable differences in the number of detected vascular loops between normoxia and the 3 week hypoxia-exposed retinas (Fig. 8), our results provide evidence for intussusceptive angiogenesis, assessed by its hallmark of loop formation (Burri et al., 2004;Patan et al., 2001), as the mechanism of microvascular network expansion in the adult retina under hypoxia.

Discussion

The principle findings of this study are that chronic systemic hypoxia results in the enlargement of vessel diameters along the arteriolar tree and induces angiogenesis in the adult mouse retina. Moreover, we provide evidence, for the first time, of intussusceptive microvascular growth as a mode of systemic hypoxia-induced angiogenesis in adult tissue. To the best of our knowledge, this study is the first to provide a detailed analysis of the vascular adaptations throughout the retinal microvasculature in response to chronic whole-body hypoxia in the adult mouse.

In addition to examining multiple time points, our study is the first to provide a detailed analysis of the retinal microvascular remodeling occurring in response to chronic systemic hypoxia in rodents. Previous work conducted in the rat has utilized stereological techniques and sectioning to investigate angiogenesis in the retinal microcirculation in response to hypoxia, which do not allow for distinction of vessel type or direct measurement of angiogenesis metrics (Shortt et al., 2004). Instead, our study utilized immunohistochemical techniques on intact, whole-mounted retinal microvascular networks to directly measure vascular length density, branch point density, and vessel diameter. Furthermore, clear evidence exists that even closely-related species can exhibit differential angiogenic responses for the same stimuli (Norrby et al., 1989; Pichiule and LaManna, 2002; Ward et al., 2007), and we found that hypoxia-induced retinal angiogenesis occurs on a different time scale than in rats (Shortt et al., 2004).

The whole-mount methods used in this study ensure that metrics of angiogenesis were obtained from the same spatial location along the hierarchy of retinal microvascular networks (i.e. vascular length density and branch point density are measured from arterioles and post-arteriolar capillaries in the superficial vascular plexus). We were able to obtain distinct measurements for each vessel type of the retinal microvascular network. This distinction of vessel type is vital to our understanding of the structural microvascular remodeling response, as we found heterogeneous remodeling throughout the networks of the superficial retina in response to hypoxia (i.e. venules did not undergo any diameter expansion).

Our data show that arteriolar diameters are increased following hypoxia, suggesting that vessel dilation (through endothelial cell stretching and distension (Dhillon et al., 1984)) or structural vessel enlargement (through perivascular cell proliferation or hypertrophy (Price and Skalak, 1998)) occurs in the retinal circulation as a result of hypoxia. Upon exposure to 10% environmental oxygen, retinal arterial P_{O2} decreases by 39%, and retinal capillary P_{O2} (a measurement more reflective of retinal tissue oxygenation) is reduced by 30% in the adult rat (Shahidi et al., 2009). Although the retina under normoxic conditions is considered relatively hypoxic with a P_{O2} of ~25 mmHg, it still has one of the highest metabolic demands of any tissue (Antonetti et al., 2006). In order to meet those demands, compensation to whole-body hypoxia in the retina appears to involve vessel diameter expansion, in an effort to normalize tissue oxygen consumption via an increase in blood flow (Shahidi et al., 2009).

A similar response to hypoxia occurs in other tissues, in an effort to restore oxygen delivery to normal values. For instance, in the adult rat brain, adaptations to 2 weeks of normobaric hypoxia involve a significant increase in blood vessel size (Miyamoto et al., 2005). Chronic

exposure to hypoxia in the adult rat also results in vessel diameter enlargement in the carotid body (attributed to endothelial stretching and distension), increasing the total surface area of blood vessel available for gas exchange (Dhillon et al., 1984). As the results of our study also indicate vessel diameter enlargement, this structural adaptation in the retina may have similar important beneficial consequences for gas exchange between the retinal circulation and tissue.

Interestingly, although vascular diameters were found to significantly increase along the arteriole component of the retinal microvascular networks, this increase in diameter was not accompanied by an increase in SMA-expressing perivascular cell investment along the length of the vascular tree. It is possible that since the retinal microvessels have particularly high pericyte coverage as compared to the microvessels of other tissue (Funk, 1997), there is no stimulus for the increased SMC coverage often involved with vessel expansion (Murfee et al., 2004; Peirce and Skalak, 2003; Van Gieson et al., 2003). Additionally, the majority of the measured increases in vessel diameter occurred in vessel orders 1, 2, and 3, which were shown to be SMA-positive in both the normoxia and hypoxia groups. We speculate that we did not observe any extension of SMA-positive cell coverage along the length of the network because the existing SMCs were capable of accommodating the hypoxia-induced adaptive response of vessel expansion.

In addition to an increase in vascular diameter, an increase in vascular length and branching in the retina was also observed after 3 weeks of hypoxia. These results are consistent with previous findings demonstrating that chronic whole-body exposure to reduced oxygen levels leads to an increase in vascular density in many tissues in adult animals. For example, in lung tissue, chronic exposure to 10% oxygen results in increased vascularity in adult rats (Howell et al., 2003). Chronic whole-body exposure to hypoxia also leads to angiogenesis in brain regions such as the cerebral cortex, hippocampus, and cerebellum in both adult mice and rats (Miyamoto et al., 2005; Ward et al., 2007). In skeletal muscles such as the diaphragm, soleus, and tibialis anterior muscles, 6 weeks of hypoxia exposure leads to increased capillary density in the adult rat (Deveci et al., 2002).

To date, no work has investigated the angiogenic mechanism behind the adaptive retinal vascular network expansion accompanying chronic hypoxia in adult mammals. Therefore, we were motivated to investigate which mode of angiogenesis (i.e. sprouting or intussusceptive angiogenesis) may produce the measured response. As we did not detect any blind-ended capillary sprouts in any of our retina samples at any time point, we next sought to test the hypothesis that intussusception, another of angiogenesis (Egginton et al., 2001), plays a role in the hypoxia-induced adaptations of the adult murine retinal circulation. Based on the significant increase in the number of vascular loops (a hallmark of intussusception (Burri et al., 2004; Patan et al., 2001)) in hypoxia-exposed retinas, our results provide evidence for intussusceptive angiogenesis as the mechanism of microvascular network expansion in the adult retina under hypoxia.

The results of this study which indicate a correlation between vessel diameter expansion and subsequent intussusceptive angiogenesis in the retina are supported by previous work which demonstrates that intussusceptive angiogenesis occurs in skeletal muscle when vessel dilation is induced through prazosin, a compound which chronically increases blood flow and hence wall shear stress (Zhou et al., 1998). Additionally, clamping of one of the dichotomous branches of an artery in the chick chorioallantoic membrane (CAM) microvasculature increases blood flow and/or pressure in its counterpart branch, resulting in the rapid formation of tissue pillars (Djonov et al., 2002). It is possible then that hemodynamic factors, such as shear stress, may induce a cascade of reactions in endothelial cells leading to pillar formation (Dome et al., 2007) and may be important regulators of intussusceptive angiogenesis in the retina. The observed vessel diameter expansion may likely reflect vessel dilation through endothelial cell

stretching and distension, rather than structural vessel enlargement through cellular proliferation, based on previous findings which attribute chronic hypoxia-induced vessel enlargement in the carotid body to endothelial cell stretching and distention (Dhillon et al., 1984) and which describe intussusceptive angiogenesis as not being primarily dependent on endothelial cell proliferation (Djonov et al., 2003; Kurz et al., 2003).

To the best of our knowledge, this study is the first to present intussusceptive angiogenesis as an adaptation to chronic systemic hypoxia in the adult retina; however, a link between local tissue hypoxia and intussusception has been previously established in the literature. Intussusceptive microvascular growth is a known hypoxia-adaptation mechanism in tumors (Dome et al., 2007). Also, in a murine model of ovarian pedicle repair, loop formation via intussusceptive angiogenesis accompanied the healing of the hypoxic tissue (Patan et al., 2001). When the two main modes of angiogenesis, sprouting and intussusceptive angiogenesis, were compared in a computational model of oxygen transport in skeletal muscle, networks undergoing intussusceptive angiogenesis were found to provide better oxygen delivery to the tissue than sprouting or control networks and resulted in the lowest volume of hypoxic tissue (Ji et al., 2006). A similar functional consequence of intussusception may be occurring in the retinal tissue of this study, whereby the new intussusceptive vascular growth provides greater surface area for gas exchange and shortens the distances over which the oxygen must diffuse.

Intussusceptive angiogenesis is known to occur in a variety of tissues in a variety of species. In addition to the developing rat lung, avian kidney, and CAM, intussusception has been revealed to occur in many organs and species during both normal and pathological microvascular growth (Djonov and Makanya, 2005; Djonov et al., 2002; Patan et al., 2001). Of particular relevance to this study, intussusceptive angiogenesis has been found to occur in the developing amphibian retina. The vascular loops presented as evidence of the progressive stages of intussusceptive growth in the amphibian retina are consistent with the results presented in this study, particularly in terms of the size and morphology of the vascular loops (Dunlop et al., 1997).

Our results are also supported by previous work which demonstrated hypoxia-induced retinal angiogenesis in the adult zebrafish (Cao et al., 2008). In the zebrafish however, retinal angiogenesis was found to proceed via capillary sprouting, not intussusceptive vascular growth as we have demonstrated occurs in mice. The marked differences between mice and zebrafish in the structure and architecture of their retinal vascular networks (Cao et al., 2008) may explain this differential mode of hypoxia-induced angiogenesis between the two species.

Although the retinal vasculature of the adult zebrafish shares some basic similarities with that of humans, such as a perivascular cell coating and endothelial cell junctions (Alvarez et al., 2007), murine retinal vascular networks are much more similar to those of humans. Both human and murine retinal vasculature contain high density microvascular networks derived from the central retinal artery and central retinal vein which radiate from the optic nerve to the periphery of the retina (Cao et al., 2008; Fruttiger, 2007; Gariano and Gardner, 2005), and therefore the findings of our study may have more relevance to humans.

Our study is the first to investigate perivascular cell coverage in hypoxia-induced retinal microvascular remodeling, and demonstrates that the intussusceptive angiogenic response is accompanied by pericyte investment of the vasculature. These findings are supported by previous analyses showing that perivascular cells are recruited during the initial and final phases of vascular pillar formation in several organs (Djonov et al., 2002). It is postulated in the literature that the recruitment of pericytes may contribute to the synthesis and subsequent stabilization of the transcapillary tissue pillar or to the maintenance of vascular structural integrity (i.e. low vascular permeability) during intussusception (Djonov et al., 2003). The

stabilization provided by the vascular support cells may contribute to the finding that the angiogenic response measured in this study does not appear to involve the pathological conditions that occur in many retinal vascular diseases, such as vessel hemorrhaging (Gariano and Gardner, 2005; Smith, 2004; Smith et al., 1994). The type of remodeling involved in chronic whole-body hypoxia then could be potentially compared to more pathological settings of retinal angiogenesis, in order to identify potential therapeutic targets or intervention strategies.

Previous work has initiated the investigation into the molecular signals governing whole-body hypoxia-induced retinal angiogenesis. Vascular endothelial growth factor receptor 2 (VEGFR2) activation and suppression of the Notch signaling pathway have been implicated in zebrafish retinal sprouting angiogenesis induced by exposure to environmental hypoxia (Cao et al., 2008), but the molecular signaling processes that govern intussusception are not well understood. There is speculation that some of the ligands and receptors involved in sprouting angiogenesis, such as Tie-2 and the angiopoietins, may play a role (Djonov and Makanya, 2005). Erythropoeitin (EPO) may also be a molecular mediator, as it has been found to induce intussusceptive microvascular growth in the CAM assay (Crivellato et al., 2004) and EPO is also known to be upregulated under hypoxia (Stockmann and Fandrey, 2006). Although hypoxia-inducible factor-1α (HIF-1α) is implicated in a variety of hypoxia-related ocular pathologies (Arjamaa and Nikinmaa, 2006) and has been shown to be upregulated in brain tissue under chronic whole-body hypoxia in mice (Shao et al., 2004), it remains unclear whether HIF-1α is involved in the type of retinal microvascular remodeling presented in our study (Arjamaa and Nikinmaa, 2006). Indeed, one of the key growth factors downstream of HIF-1α activation, VEGF, appears not to be required for intussusceptive angiogenesis (Djonov et al., 2001), possibly because intussusceptive angiogenesis is achieved in the virtual absence of endothelial cell proliferation (Djonov et al., 2003; Djonov and Makanya, 2005; Kurz et al., 2003). Therefore, further work is needed to investigate the molecular mechanisms involved in murine chronic systemic hypoxia-induced microvascular remodeling. The results derived from this work allow for the possible experimental use of genetically-altered mouse strains to elucidate the molecular mechanisms of hypoxic adaptation.

In summary, this study is the first to provide a detailed examination of chronic whole-body hypoxia-induced angiogenesis and microvascular remodeling in the adult mouse retina. Our results demonstrate that vessels of the arteriolar tree undergo diameter expansion and that angiogenesis occurs in the superficial retina in response to chronic systemic hypoxia. Furthermore, this study identifies, for the first time, intussusceptive angiogenesis as a mechanism of microvascular growth in the retina resulting from chronic hypoxia exposure. This work contributes to our understanding of the retinal vascular adaptations made in response to hypoxia, and ultimately, the findings of this study may be utilized for the discovery of cellular or molecular targets for treating certain features of proliferative vasculopathies that are downstream of hypoxia.

Acknowledgments

This work was funded by a grant from the National Institutes of Health (R01 HL082838-02 to Shayn M. Peirce). The authors would like to acknowledge the Tissue Histology Core at the University of Virginia for providing the whole-eye cross-sections for this study.

References

Alvarez Y, et al. Genetic determinants of hyaloid and retinal vasculature in zebrafish. BMC Dev Biol 2007;7:114. [PubMed: 17937808]

Antonetti DA, et al. Diabetic retinopathy: seeing beyond glucose-induced microvascular disease. Diabetes 2006;55:2401–11. [PubMed: 16936187]

Arjamaa O, Nikinmaa M. Oxygen-dependent diseases in the retina: role of hypoxia-inducible factors. Exp Eye Res 2006;83:473–83. [PubMed: 16750526]

Burri PH, Djonov V. Intussusceptive angiogenesis--the alternative to capillary sprouting. Mol Aspects Med 2002;23:S1–27. [PubMed: 12537983]

Burri PH, et al. Intussusceptive angiogenesis: its emergence, its characteristics, and its significance. Dev Dyn 2004;231:474–88. [PubMed: 15376313]

Campochiaro PA. Retinal and choroidal neovascularization. J Cell Physiol 2000;184:301–10. [PubMed: 10911360]

Cao R, et al. Hypoxia-induced retinal angiogenesis in zebrafish as a model to study retinopathy. PLoS ONE 2008;3:e2748. [PubMed: 18648503]

Claxton S, Fruttiger M. Oxygen modifies artery differentiation and network morphogenesis in the retinal vasculature. Dev Dyn 2005;233:822–8. [PubMed: 15895398]

Crivellato E, et al. Recombinant human erythropoietin induces intussusceptive microvascular growth in vivo. Leukemia 2004;18:331–6. [PubMed: 14671634]

Das A, McGuire PG. Retinal and choroidal angiogenesis: pathophysiology and strategies for inhibition. Prog Retin Eye Res 2003;22:721–48. [PubMed: 14575722]

Deveci D, et al. Chronic hypoxia induces prolonged angiogenesis in skeletal muscles of rat. Exp Physiol 2002;87:287–91. [PubMed: 12089595]

Dhillon DP, et al. The enlarged carotid body of the chronically hypoxic and chronically hypoxic and hypercapnic rat: a morphometric analysis. Q J Exp Physiol 1984;69:301–17. [PubMed: 6729019]

Djonov V, et al. Vascular remodelling during the normal and malignant life cycle of the mammary gland. Microsc Res Tech 2001;52:182–9. [PubMed: 11169866]

Djonov V, et al. Vascular remodeling by intussusceptive angiogenesis. Cell Tissue Res 2003;314:107–17. [PubMed: 14574551]

Djonov V, Makanya AN. New insights into intussusceptive angiogenesis. EXS 2005:17–33. [PubMed: 15617468]

Djonov VG, et al. Optimality in the developing vascular system: branching remodeling by means of intussusception as an efficient adaptation mechanism. Dev Dyn 2002;224:391–402. [PubMed: 12203731]

Dome B, et al. Alternative vascularization mechanisms in cancer: Pathology and therapeutic implications. Am J Pathol 2007;170:1–15. [PubMed: 17200177]

Dunlop SA, et al. Changing patterns of vasculature in the developing amphibian retina. J Exp Biol 1997;200:2479–92. [PubMed: 9343858]

Egginton S, et al. Unorthodox angiogenesis in skeletal muscle. Cardiovasc Res 2001;49:634–46. [PubMed: 11166277]

Engelson ET, et al. The microvasculature in skeletal muscle. I. Arteriolar network in rat spinotrapezius muscle. Microvasc Res 1985;30:29–44. [PubMed: 4021836]

Fruttiger M. Development of the retinal vasculature. Angiogenesis 2007;10:77–88. [PubMed: 17322966]

Funk RH. Blood supply of the retina. Ophthalmic Res 1997;29:320–5. [PubMed: 9323723]

Gariano RF, Gardner TW. Retinal angiogenesis in development and disease. Nature 2005;438:960–6. [PubMed: 16355161]

Gerhardt H, Betsholtz C. Endothelial-pericyte interactions in angiogenesis. Cell Tissue Res 2003;314:15–23. [PubMed: 12883993]

Hansen-Smith F, et al. Growth of arterioles precedes that of capillaries in stretch-induced angiogenesis in skeletal muscle. Microvasc Res 2001;62:1–14. [PubMed: 11421656]

Howell K, et al. Chronic hypoxia causes angiogenesis in addition to remodelling in the adult rat pulmonary circulation. J Physiol 2003;547:133–45. [PubMed: 12562951]

Ji JW, et al. A computational model of oxygen transport in skeletal muscle for sprouting and splitting modes of angiogenesis. J Theor Biol 2006;241:94–108. [PubMed: 16388825]

Kurz H, et al. Angiogenesis and vascular remodeling by intussusception: from form to function. News Physiol Sci 2003;18:65–70. [PubMed: 12644622]

Linsenmeier RA, et al. Retinal hypoxia in long-term diabetic cats. Invest Ophthalmol Vis Sci 1998;39:1647–57. [PubMed: 9699554]

Miyamoto O, et al. Vascular changes in the rat brain during chronic hypoxia in the presence and absence of hypercapnia. Acta Med Okayama 2005;59:135–43. [PubMed: 16155639]

Murfee WL, et al. Cell proliferation in mesenteric microvascular network remodeling in response to elevated hemodynamic stress. Ann Biomed Eng 2004;32:1662–6. [PubMed: 15675679]

Norrby K, et al. Mast-cell secretion and angiogenesis, a quantitative study in rats and mice. Virchows Arch B Cell Pathol Incl Mol Pathol 1989;57:251–6. [PubMed: 2474890]

Palmer LA, et al. Hypoxia induces type II NOS gene expression in pulmonary artery endothelial cells via HIF-1. Am J Physiol 1998;274:L212–9. [PubMed: 9486205]

Patan S, et al. Vascular morphogenesis and remodeling in a model of tissue repair: blood vessel formation and growth in the ovarian pedicle after ovariectomy. Circ Res 2001;89:723–31. [PubMed: 11597996]

Peirce SM, et al. Spatial and temporal control of angiogenesis and arterialization using focal applications of VEGF164 and Ang-1. Am J Physiol Heart Circ Physiol 2004;286:H918–25. [PubMed: 14604856]

Peirce SM, Skalak TC. Microvascular remodeling: a complex continuum spanning angiogenesis to arteriogenesis. Microcirculation 2003;10:99–111. [PubMed: 12610666]

Pichiule P, LaManna JC. Angiopoietin-2 and rat brain capillary remodeling during adaptation and deadaptation to prolonged mild hypoxia. J Appl Physiol 2002;93:1131–9. [PubMed: 12183511]

Price RJ, Skalak TC. Arteriolar remodeling in skeletal muscle of rats exposed to chronic hypoxia. J Vasc Res 1998;35:238–44. [PubMed: 9701707]

Saint-Geniez M, et al. The msr/apj gene encoding the apelin receptor is an early and specific marker of the venous phenotype in the retinal vasculature. Gene Expr Patterns 2003;3:467–72. [PubMed: 12915314]

Shahidi M, et al. Three-dimensional mapping of chorioretinal vascular oxygen tension in the rat. Invest Ophthalmol Vis Sci 2009;50:820–5. [PubMed: 18824736]

Shao R, et al. Increase of SUMO-1 expression in response to hypoxia: direct interaction with HIF-1alpha in adult mouse brain and heart in vivo. FEBS Lett 2004;569:293–300. [PubMed: 15225651]

Shortt AJ, et al. Chronic systemic hypoxia causes intra-retinal angiogenesis. J Anat 2004;205:349–56. [PubMed: 15575883]

Smith LE. Pathogenesis of retinopathy of prematurity. Growth Horm IGF Res 2004;14:S140–4. [PubMed: 15135797]

Smith LE, et al. Oxygen-induced retinopathy in the mouse. Invest Ophthalmol Vis Sci 1994;35:101–11. [PubMed: 7507904]

Stockmann C, Fandrey J. Hypoxia-induced erythropoietin production: a paradigm for oxygen-regulated gene expression. Clin Exp Pharmacol Physiol 2006;33:968–79. [PubMed: 17002676]

Taylor AC, et al. EphB4 expression along adult rat microvascular networks: EphB4 is more than a venous specific marker. Microcirculation 2007;14:253–67. [PubMed: 17454677]

Van Gieson EJ, et al. Enhanced smooth muscle cell coverage of microvessels exposed to increased hemodynamic stresses in vivo. Circ Res 2003;92:929–36. [PubMed: 12663481]

Wangsa-Wirawan ND, Linsenmeier RA. Retinal oxygen: fundamental and clinical aspects. Arch Ophthalmol 2003;121:547–57. [PubMed: 12695252]

Ward NL, et al. Cerebral angiogenic factors, angiogenesis, and physiological response to chronic hypoxia differ among four commonly used mouse strains. J Appl Physiol 2007;102:1927–35. [PubMed: 17234796]

Zhou AL, et al. Capillary growth in overloaded, hypertrophic adult rat skeletal muscle: an ultrastructural study. Anat Rec 1998;252:49–63. [PubMed: 9737744]

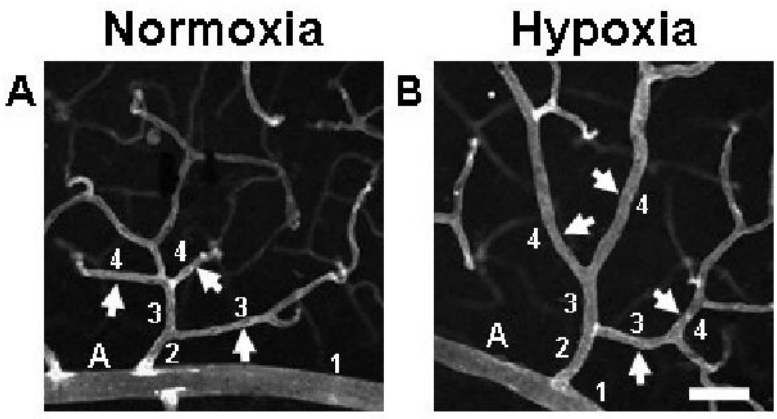

FIGURE 1.

Exposure to whole-body hypoxia resulted in an apparent increase in the diameters of arterioles and post-arteriole capillaries of murine superficial retinal microvascular networks. High magnification (20×) confocal images obtained from retinal whole-mounts labeled with lectin were used to examine hypoxia-induced changes in vessel diameter throughout the microvascular tree. Representative arterioles and capillaries (arrows) downstream of main arterioles (labeled 'A') exhibit increased diameters in animals exposed to systemic hypoxia **(B)**, as compared with age-matched normoxic controls **(A)**. To categorize vessels so that diameters could be compared for vessels of similar phenotype and relative location in the network, main arterioles were defined as vessel order 1, and sequential orders were assigned progressively downstream, incrementing at branch points at which two vessels of the same order joined (see numbers in figure) (Peirce et al., 2004). Scale bar = 50 μm.

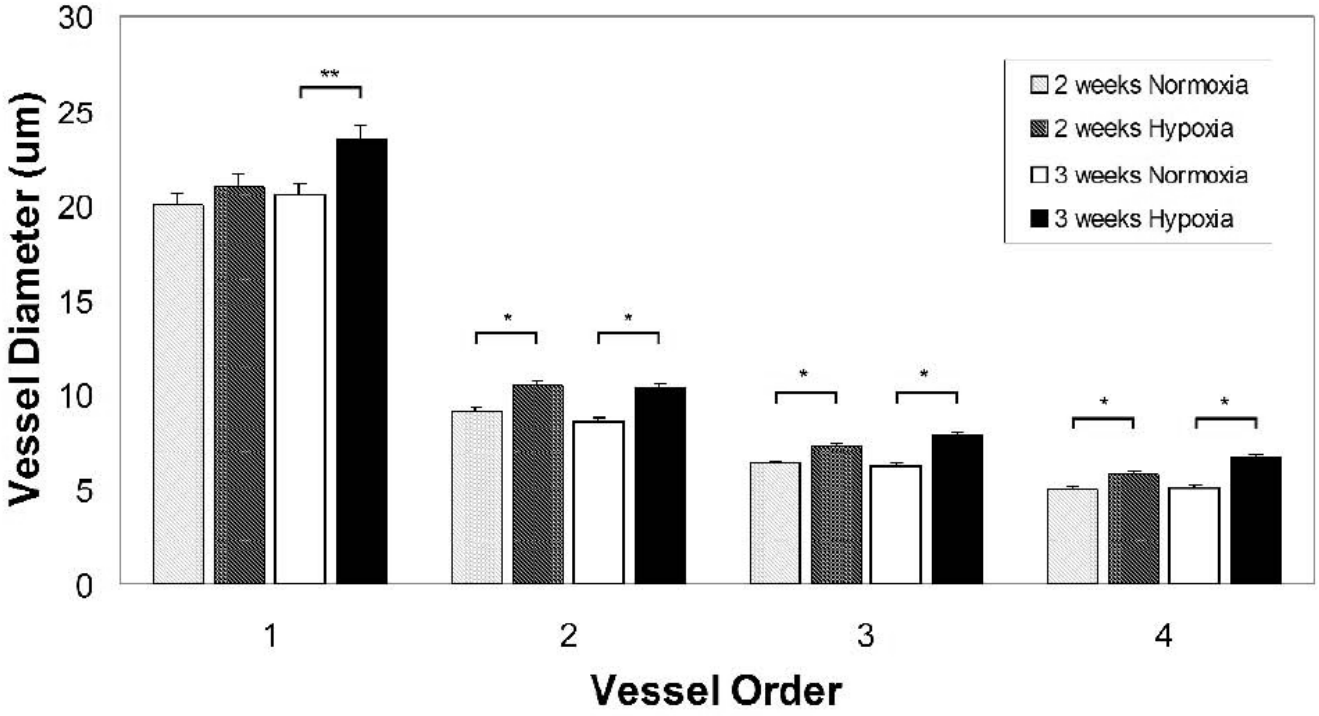

FIGURE 2.

Quantification of vessel diameters in superficial retinal microvascular networks revealed the presence of microvascular remodeling after hypoxia exposure. Vessels were categorized so that diameters could be compared for vessels of similar phenotype and relative location in the network, as demonstrated in Fig. 1. Quantification of retinal vessel diameters showed that exposure to 3 weeks of hypoxia resulted in a significant increase in the vessel diameters of main central arterioles ($p = 0.003$) as well as downstream arterioles (majority found to be of vessel order 2 and 3) and capillaries (majority found to be of vessel order 4) ($p < 0.001$). A significant increase in vessel diameters was also measured after 2 weeks of hypoxia for vessel orders 2, 3, and 4 ($p < 0.001$). The increase in the central arteriole diameter (vessel order 1) was not significant after 2 weeks of hypoxia exposure.

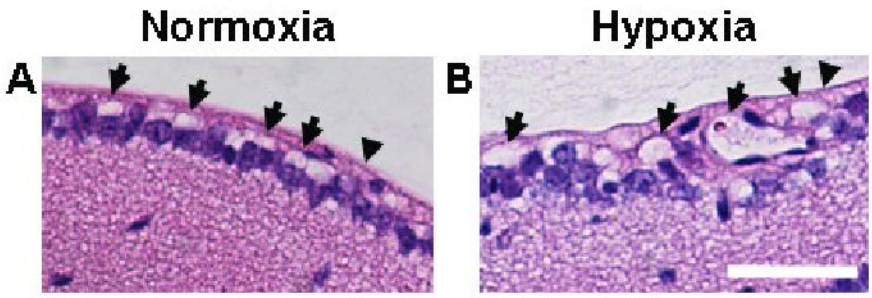

FIGURE 3.

Whole-eye sections were taken from 13 wk-old mice and were stained using H&E. Whole-eye 5 μm-thick sections from mice exposed to normoxia **(A)** or hypoxia **(B)** further demonstrated diameter enlargement in vessels of the superficial retina (arrows) after 3 weeks of hypoxia exposure relative to normoxic controls. In addition, whole-eye sections indicated that the angiogenic response induced by chronic whole-body hypoxia did not involve the formation of preretinal neovascular tufts that penetrate the inner limiting membrane (arrowheads). Scale bar = 50 μm.

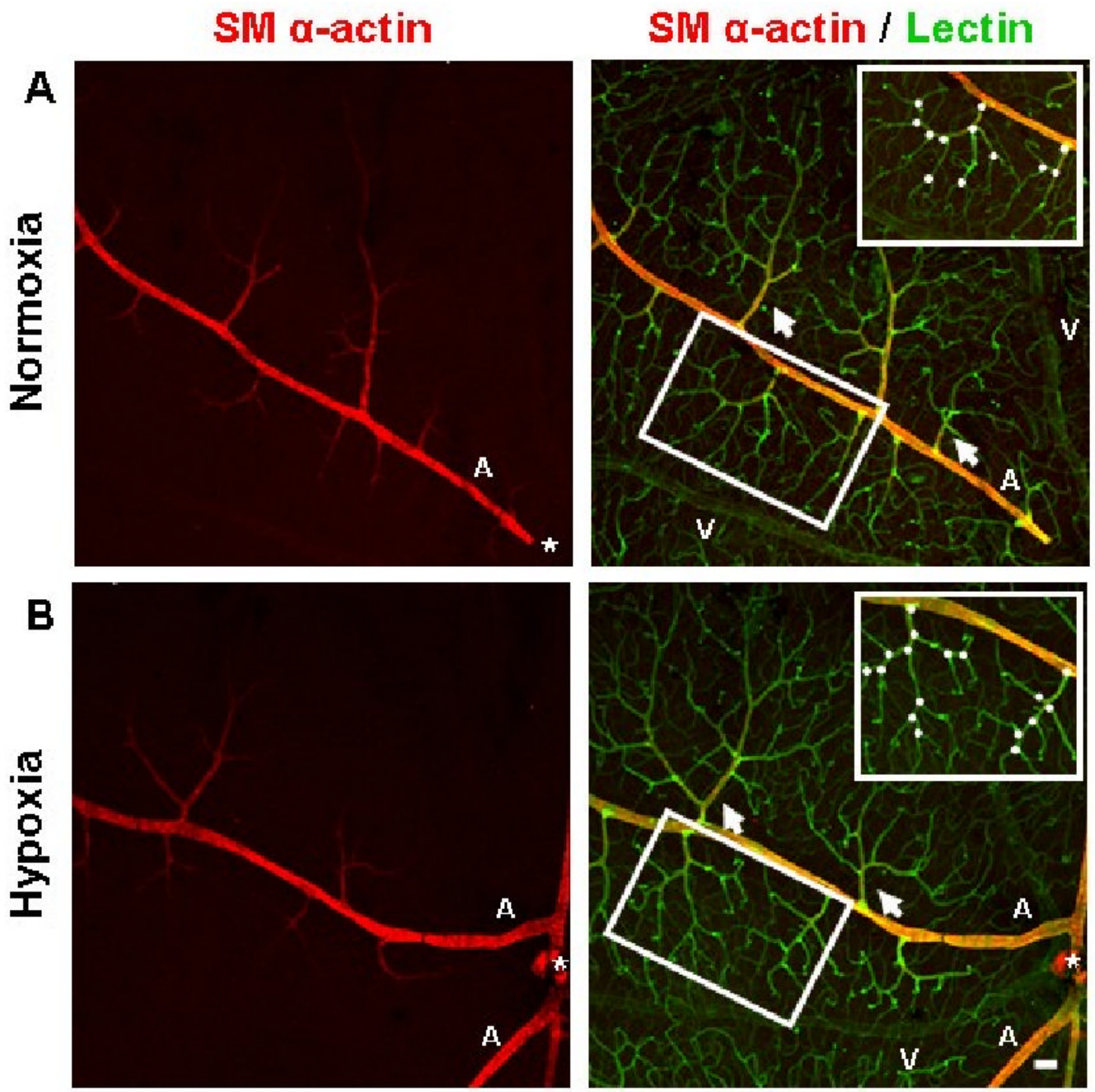

FIGURE 4.

Immunohistochemistry performed on whole-mounted retinal tissue qualitatively showed that the vascular networks of the superficial retina underwent angiogenesis as a result of systemic hypoxia. Representative superficial post-arteriole vascular networks (arrows) labeled with lectin (green) from animals exposed to 3 weeks of hypoxia appear to exhibit an increased degree of vascularization **(B)** compared to retinal vascular networks from animals exposed to normoxia **(A)**. Representative post-arteriole vascular networks (insets) demonstrate an increased amount of branch points (white circles) in hypoxia-exposed tissue **(B)** compared to networks from normoxia-exposed animals **(A)**. Both upstream mother vessel and downstream daughter vessel were required to be located in the same confocal plane as the post-arteriole

superficial network in order to be counted as a branch point. In the mouse retina, the main arterioles (labeled ‘A’) and venules (labeled ‘V’) of the superficial retina extend radially from the optic nerve (*) and are distributed alternately. Arteriole vessel identity was determined by the presence of SMA immunostaining (red). SMA investment appeared to be similar between normoxic and hypoxia-exposed retinas. Scale bar = 50 μm.

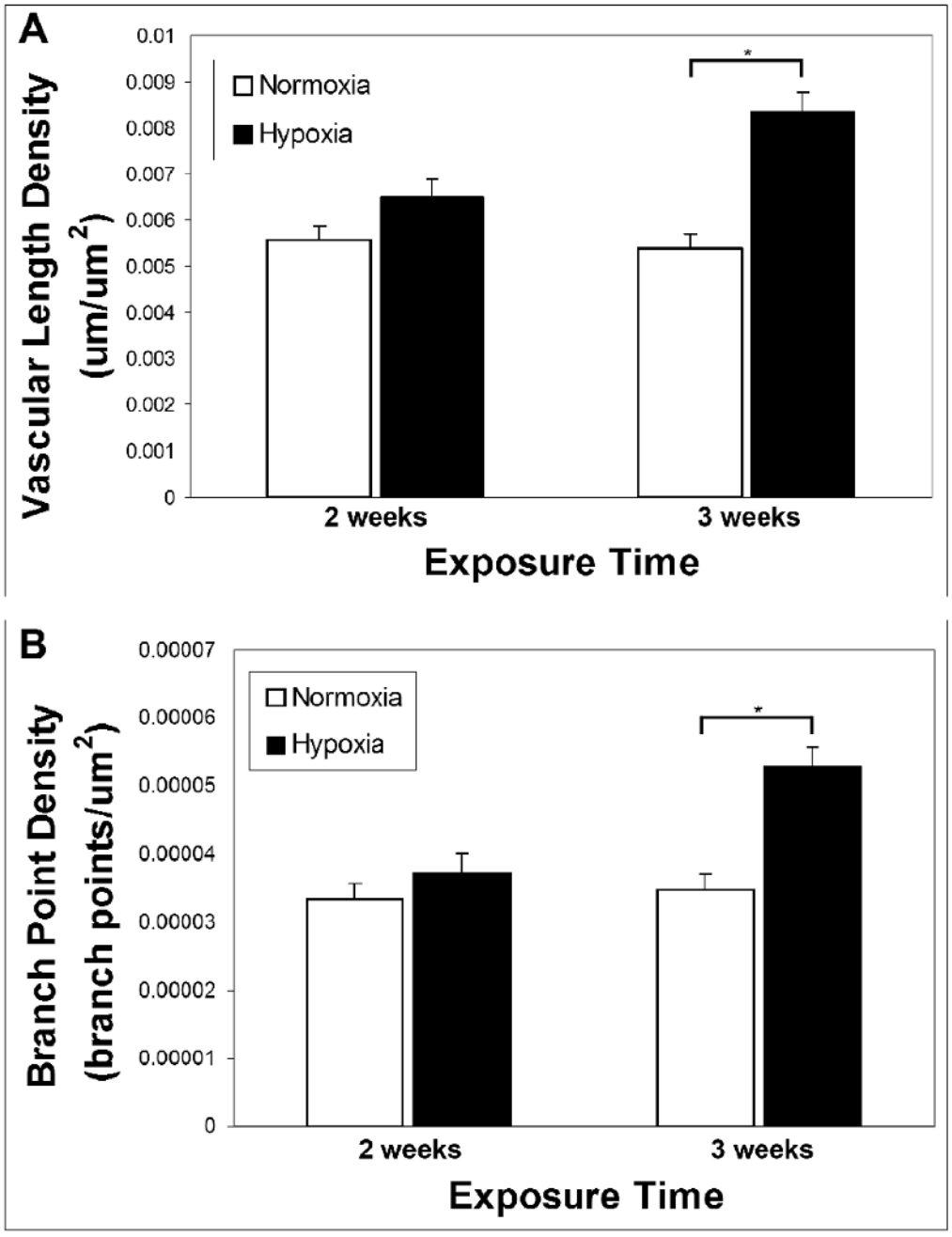

FIGURE 5.

Quantification of vascular length density and branch point density in the superficial retinal microvasculature demonstrated that chronic systemic hypoxia resulted in intra-retinal angiogenesis. Vascular length density was measured in whole-mounted, immunolabeled retinal tissue after 2 and 3 weeks of hypoxia exposure **(A)**. A significant increase in the vascular length density of the superficial retinal microvasculature was seen after 3 weeks of hypoxia ($p < 0.001$). After only 2 weeks of hypoxia, the increase in vascular length density was not significant. Similarly, no significant increase was seen in branch point density after 2 weeks of hypoxia, but 3 weeks of hypoxia exposure resulted in a significant increase in branch point density ($p < 0.001$) **(B)**.

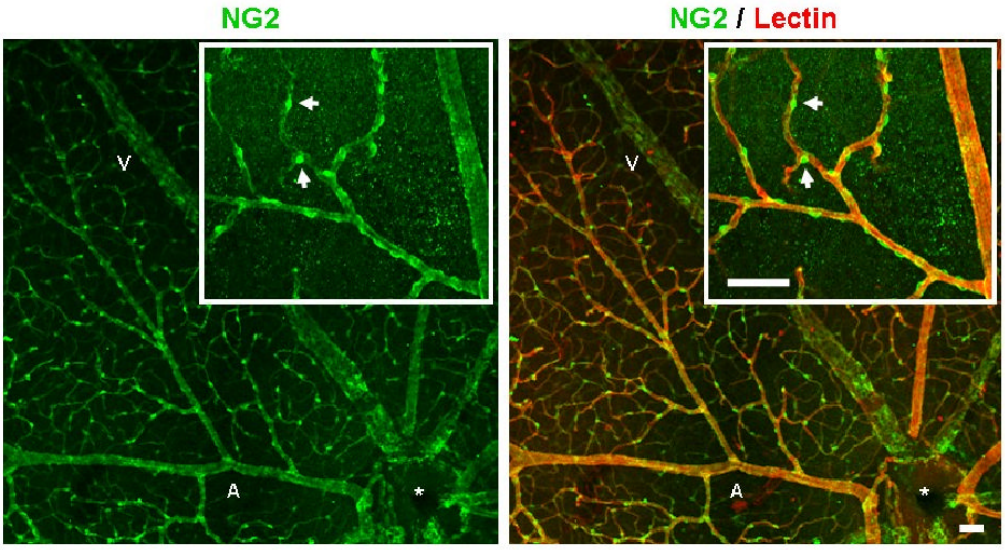

FIGURE 6.

Co-immunolabeling for pericyte marker NG2, as well as lectin, demonstrated the extensive pericyte coverage of retinal microvascular networks after 3 weeks of hypoxia exposure. All retinal microvessels labeled with lectin (red) were heavily invested by NG2-expressing pericytes (green). High magnification revealed pericyte wrapping of the main arteriole and post-arteriole capillaries (inset). Scale bar = 50 μm. Normoxia-exposed retinas displayed similar pericyte coverage density (data not shown).

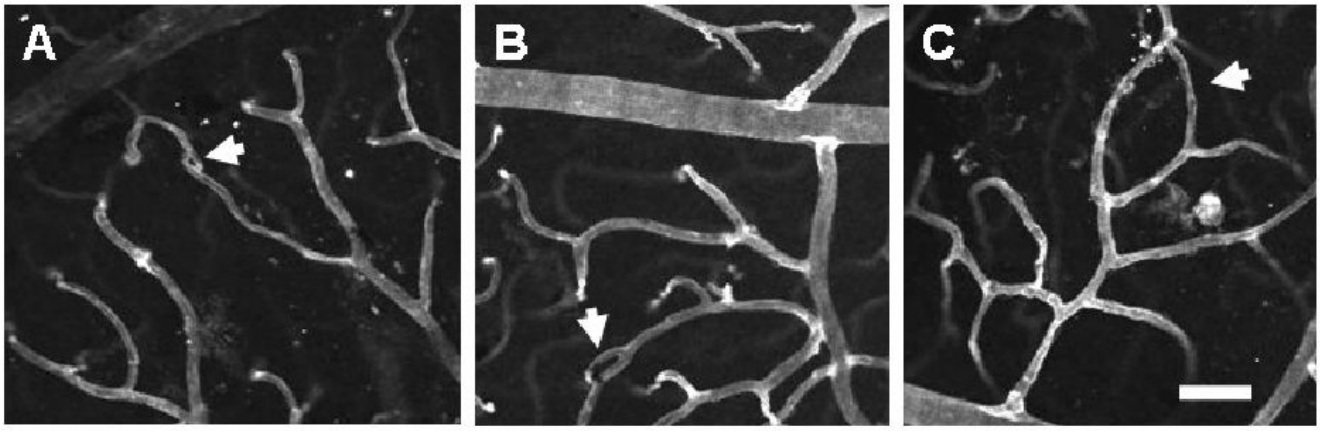

FIGURE 7.

Exposure to whole-body hypoxia for 3 weeks results in vascular loop formation in the superficial networks of the adult mouse retina. High magnification (20×) confocal images obtained from retinal whole-mounts labeled with lectin (white) were used to examine the presence of vascular loops (arrows). Representative vascular loops illustrate the wide range of loop sizes observed in hypoxia-exposed retinas, which appear to correspond to the progressive stages of intussusceptive microvascular growth (Burri and Djonov, 2002), from the initial formation of a tissue pillar **(A)** to its subsequent elongation **(B)** and expansion to form larger vascular loops **(C)**. The smallest loops detected **(A)** corresponded to the size and morphology of early tissue pillars previously identified in the developing amphibian retina (Dunlop et al., 1997). Scale bar = 50 μm.

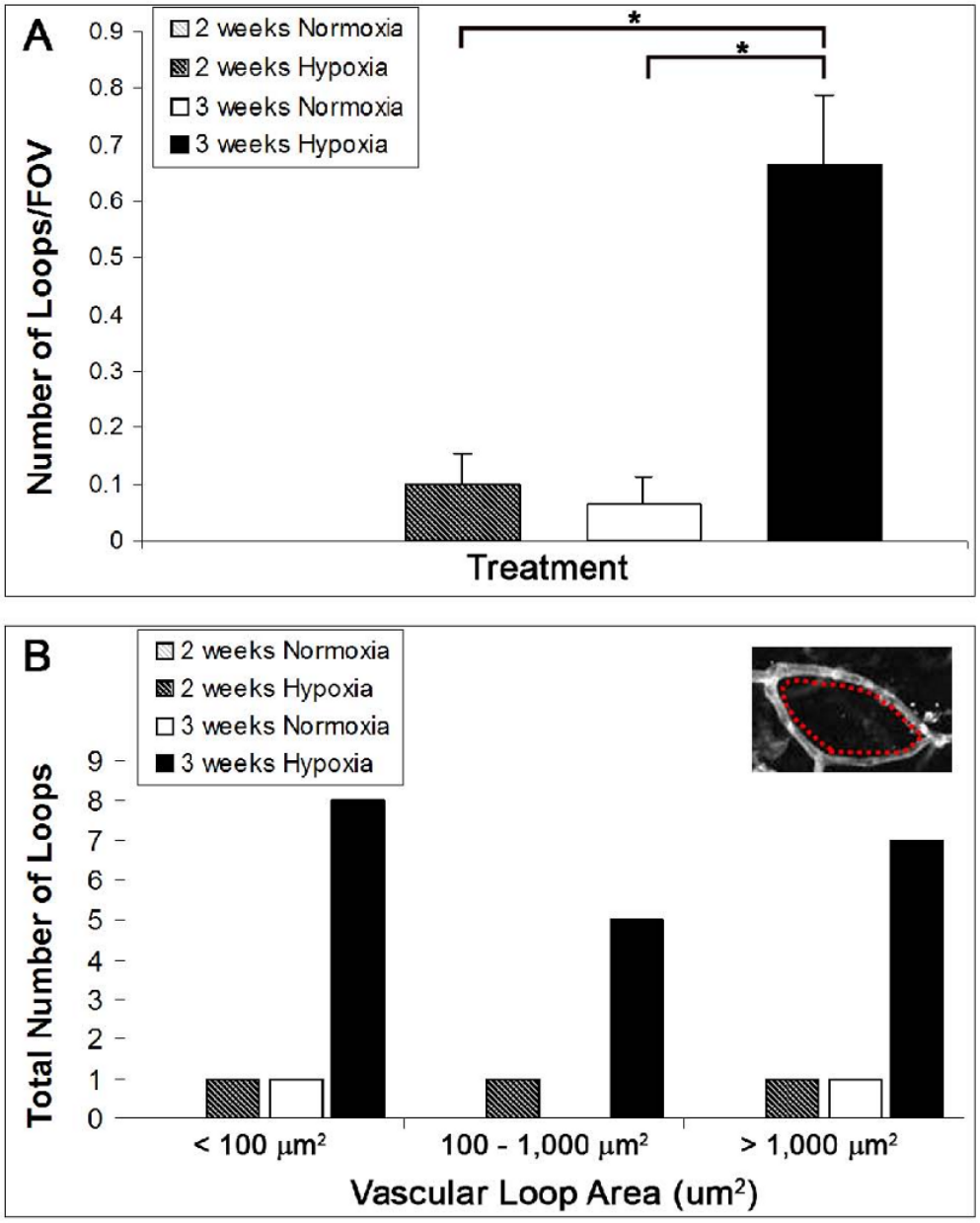

FIGURE 8.

Quantification of the number and size of vascular loops detected in superficial retinal networks revealed that 3 weeks of chronic systemic hypoxia resulted in the formation of loops, a hallmark of intussusceptive angiogenesis (Dunlop et al., 1997; Patan et al., 2001). The number of vascular loops in representative FOV (20×) from immunolabeled superficial retinal networks was recorded. Retinas exposed to hypoxia for 3 weeks were found to have a significantly greater number of loops per FOV than age-matched normoxic controls ($p \leq 0.001$). Also, the formation of vascular loops was significantly greater after 3 weeks of hypoxia exposure as compared to only 2 weeks of hypoxia exposure ($p \leq 0.001$) **(A)**. Note that the values for the 2 weeks normoxia control group were so low that they are not visible. The area encompassed by each vascular loop was measured (inset, red dashes) and a histogram of loop size distribution was generated **(B).** Out of the 30 FOV examined per treatment group, only 2 loops were detected for the 3

week normoxia-exposed retinas. Only 3 loops were detected in the 2 week hypoxia-exposed retinas, and their sizes were evenly distributed among the loop size categories. In contrast, 20 loops were measured in the 3 week hypoxia-exposed retinas, and their sizes were nearly evenly distributed among the three loop size categories (< 100 μm^2, 100 – 1,000 μm^2, and > 1,000 μm^2) **(B).**